Original article

Experimental investigation of helical gear tooth crack location and depth detection using moving average method on transmission error

Mohsen Rezaei ⓘ, **Mehrdad Poursina** ⓘ **and Ehsan Rezaei**

Abstract

Gear systems are the most useful and essential power transmission systems in the high-speed industry due to their accuracy. It is necessary to make sure that these systems work without defects such as tooth cracks. Therefore, detecting the location and depth of cracks in gear systems is very important. In this research, a new approach is proposed to detect the crack location, and accordingly, some statistical indicators are used to estimate the crack depth in the helical gear tooth. To this end, after explaining the helical gear mesh stiffness and tooth-root crack modeling, the helical gear pair dynamic is modeled. Then, the vibration data of a helical gear system is obtained by an experimental test rig, and the moving average method is undertaken to precisely detect the crack location. The crack depth ratio is estimated using the crest factor, impulse factor, clearance factor, and S_r and S_α which are applied to the simulation results and the experimental signal. According to these results, the crest factor, impulse factor, and clearance factor calculated the crack depth ratio with a good agreement, and the indicators S_r and S_α estimated it with a more significant error. Also, the average of estimated values is calculated, indicating a better result than each indicator alone.

Introduction

Gear systems regarding accuracy, efficiency, and life spans are the most common and applicable systems for power transmission in the industry. Among the existing gear systems, helical gear systems are mostly used in the industry due to their high accuracy and speed. Any kind of defect, such as spall, pitting, and cracks, can reduce their efficiency and increase vibration and noise. Therefore, due to the mentioned reasons, a lot of attention is paid to detect gear systems' defects. Tooth root crack is one of the common flaws in gear systems, and this type of defect can quickly advance and make the power transmission system stop. On the other hand, finding the crack's position and its depth can save time and reduce the costs. Many diagnostic methods and data processing techniques for defect detection in gear systems, such as some statistical indicators, time synchronous averaging (TSA), and residual signal method, were used.[1]

Sait and Sharf-Eldeen[2] presented a review of several methods and indicators for monitoring the status of vibration-based gearboxes such as crest factor, energy ratio (ER), energy operator, root mean square (RMS), kurtosis, TSA, FM0, NA4, NA4*, FM4, FM4*, M6A, M6A*, M8A, M8A*, NB4, NB4*, NP4, difference signal, residual signal, bandpass mesh signal, STFT, wavelet transform, and Wigner–Ville distribution. Alkhadafe et al.[3] used various statistical indicators in the time and frequency domains of the vibration signal obtained from sensors to monitor the helical gear's condition. They evaluated statistical indicators such as mean, standard deviation (STD), variance, RMS, abs mean, skewness, kurtosis, and impulse factor in various sensors

Department of Mechanical Engineering, Faculty of Engineering, University of Isfahan, Isfahan, Iran

Corresponding author:
Mehrdad Poursina, Department of Mechanical Engineering, University of Isfahan, Hezar, Jarib Street, Isfahan 81746-7344, Islamic Republic of Iran.
Email: poursina@eng.ui.ac.ir

applied to their test gearbox. Further researches can be found in the literature.[4,5]

Jardine et al.,[6] Barszcz et al.,[7] and Dalpiaz et al.[8] also exerted time-synchronous averaging (TSA) in their researches. Braun[9] again scrutinized the TSA method and the other averaging approaches including moving average, exponential averaging, running average, Comb Filters, and frequency response function, a parallel technique through a comparative process.

Combet et al.[10] used degradation techniques to calculate the residual signal to detect local gear error using the raw vibration signal obtained from an experimental setting. Another application of amplitude and phase demodulation can be found in the research.[9] Mohammad et al.[11] calculate the gear pair's mesh stiffness with a tooth root crack and dynamically model the one-stage gear system using various models, including 6 degrees of freedom (DOF), 8 DOF, and 12 DOF dynamic models. Then, they showed the effects of different crack lengths on the vibration of their system and calculated the residual signal. They used three statistical indicators, including RMS, kurtosis, and crest factor, to diagnose tooth crack. The other researchers utilized the residual signals for crack diagnosis.[9,10]

Amarnath and Krishna[12] applied the empirical mode decomposition (EMD) method and statistical parameters on vibration and acoustic signals to detect a local defect in helical gears. They removed different percentages of teeth and used experimental data to investigate the effect of several simultaneous processes on statistical parameters.

Assaad et al.[13] examined the status of a multi-stage gearbox in an experimental test using TSA, autoregressive (AR) model, and condition indicators on the TSA signal from the gearbox's vibration. More applications of the AR model can be found in the literature.[14–16]

Furch et al.[17] using statistical indicators such as RMS and crest factor and conversion of vibration signal from time range to frequency range by Fourier transformation on detected vibration signal of a four-speed gearbox to diagnose a four-speed gearbox faults such as gear tooth breakage.

Wu et al.[18] used analytical and finite element methods (FEMs) to model tooth cracks in the gear pair's mesh stiffness. They analyzed the fault characteristics of the simulated and experimental vibration signal of the one-stage gear system.

Liang et al.[19] used a series of fixed windows according to the ring gear's teeth number in a planetary gearbox. They applied average and RMS indicators in each windowed part of the signal obtained by an experimental rig test for gear tooth fault detection. Other uses of the window functions in gear fault detection can be seen in the literature.[20–24]

Rezaei et al.[25] used a new method relying on the transmission error ratio to investigate the detection possibility of two cracks in helical gear teeth in various situations of cracks positions, depths, and lengths. Mohammed and Rantatalo[26] reviewed the literature on gear fault models such as tooth spalling, pitting, root cracks, and dynamic modeling for gear defect detection. Luo et al.[27] investigated tooth spalling defects' effect on the dynamic response and performance of the planetary gear system. They also considered sliding friction between teeth in their model.

Recently, Chen et al.[28] presented a time series model-based method for gear tooth crack detection and severity assessment under random speed variation. They used the linear parameter varying AR model and refined B-splines to predict and solve their dynamic equations. They also used an experimental setup with two helical gears with 50 and 100% (broken) tooth root cracks.

Chen et al.[29] studied the vibration feature evolution of a locomotive with tooth root crack propagation of a gear transmission system. They applied a complex dynamic model for modeling their motors' system, gear pairs, springs, mass, and dampers. They considered non-uniformly distributed tooth crack and used energy equations to determine the mesh stiffness. They used the TSA method and kurtosis, RMS, CF, M6A, M8A, etc., indexes in their signal processing procedure.

In the previous research, the main focus has been on detecting the crack location, and most of them aimed to study the spur gear pair. According to some experimental results, the traditional methods, such as residual signal, cannot determine the cracked tooth. So, it seems necessary to propose a new way to find out the cracked tooth and diagnose the crack depth ratio in helical gear pair to have the vision to determine a schedule for fixing and replacement.

In this research, the helical gear dynamic system and the crack effect on its mesh stiffness are modeled. Then, the vibration signal of a helical gear system is obtained by an experimental test rig, and the moving average method is used to find out the crack location. Then, using some statistical indicator plots obtained by dynamic simulation, the crack depth ratio is detected. Finally, the accuracy of each indicator in this experimental study is discussed.

Helical gear pair experimental test rig

The used helical gear pair experimental test rig and its schematic structure plan are presented in Figure 1. As shown in this figure, the electric power is inserted into the inverter to adjust the power supply and control the electric motor speed. Then, the electric motor is coupled with a one-stage gearbox that the two encoders are connected to the ends of its input and output shafts. The power is transferred to a generator by two double-row pulleys and two belts. The generator electric power is dissipated by a resistance used to increase the temperature of a water tank.
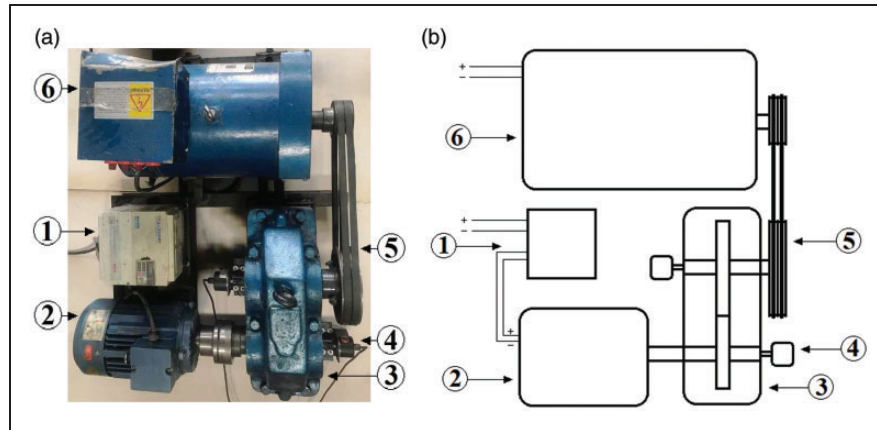
Figure 1. Helical gear pair experimental test rig (a) real photo and (b) schematic structure plan: (1) inverter; (2) electric motor; (3) one-stage gearbox; (4) encoder; (5) double-row pulley; (6) generator.

Table 1. Helical gear pair parameters.

Parameter	Pinion	Gear
Normal module (mm)	3	3
Normal pressure angle (°)	20	20
Helix angle (°)	15	15
Face width (mm)	20	20
Teeth number	44	59
Internal radios (mm)	25	30
Young's modulus (GPa)	68.9	68.9
Poison's ratio	0.3	0.3
Mass (kg)	0.677	1.259
Mass moment of inertia (g m^2)	1.774	5.808
Rotation speed (r/min)	1000	746
Bearings radial stiffness ($\frac{kN}{mm}$)	23.87	46.922
Bearings axial stiffness ($\frac{kN}{mm}$)	0.951	2.079
Motor power (kW)	2.7	
Damping ratio	1	
Maximum geometric transmission error: e_0 (mm)	0.01	

The experimental test rig system's parameters values, on which all calculations of this research are based, are listed in Table 1.

Helical gear mesh stiffness and crack modeling

Mesh stiffness

Dynamic modeling of a pair of helical gears is divided into three steps. The first step involves the analytical calculation of the helical gear pair's mesh stiffness that changing over time. The second step is determining the governing dynamic equations of the system using Newton's second law. Finally, the governing dynamic equations in the field of time are solved, and the responses of the system are achieved. In this section, an analytical calculation of the mesh stiffness of a helical gear pair is discussed. According to the potential energy method, the spur gear tooth is considered a cantilever beam.[4] Then, the axial, bending, and shear stiffness of the beam can be calculated analytically, and the teeth at their point of contact have a Hertzian stiffness.[4] The gear body, similar to a beam base, has a stiffness known as fillet-foundation stiffness. Therefore, the spur gear mesh's stiffness includes nine parts, axial, bending, shear, and fillet-foundation stiffness for each gear and their Hertzian contact stiffness.[30] The contact model between the teeth in pair of helical gears is not like spur gears. The contact line with the length of zero stars at the time of teeth contact in pair of helical gears. It gradually increases to the maximum, and finally, their contact line decreases to zero. As the contact models between teeth of spur and helical gears are different, it leads to the distinct feature of vibration. Therefore, the mesh stiffness calculation of helical gear and spur gears is not the same.[30]

Nonetheless, when the helical tooth is divided into several thin independent slices with a small thickness, it can be considered as several consecutive spur teeth that come in to contact one after one. It should be noted that there is not a connection between the slices. In other words, the shear effect between the cuts is neglected. This assumption causes error in the results, which is generally very small for gears with a thin face and a low helix angle.[30] According to our practical research for the helix angles up to 15° with a face width up to 10 multiple of gear module, the difference between the mesh stiffness calculated by this analytical method and the values obtained by the FEM remains under 5%. By stacking up the whole spur gear slices' mesh stiffness with particular angular spacing, we can efficiently compute the helical gear mesh stiffness.

Crack modeling

The crack effectiveness must be seriously considered on the helical gear pair mesh stiffness when a crack is

in the tooth root. For this purpose, a crack is generated by a wire-cut machine in the pinion tooth root (Figure 2(a)), and its equivalent crack path in gear thickness is depicted in Figure 2(b). Crack depth is considered constant in each slice to model the effectiveness of variable crack depth. The limit line method is utilized to reduce the tooth stiffness.[30]

The continuous line shows the individual stiffness of a healthy tooth pair, and the dashed line illustrates the stiffness of a teeth pair with a cracked pinion tooth. As can be seen in Figure 3, the contact line length is zero when teeth are at the beginning of contact. Then, it increases to point (b). The value is constant between points (b) and (c). Then, it decreases to zero as soon as the teeth lose their contact. The difference between healthy and defective teeth mesh stiffness is displayed in this figure.

.Helical gear pair dynamic modeling

In this section, a 6-DOF helical gear pair is considered as presented in the study of Wan et al.[30] as shown in Figure 4. The dynamic equations governing this system are extracted according to equations (1) to (6). The friction force can be neglected between the contacted teeth in the x-direction with adequate lubrication

$$I_p\ddot{\theta}_p = -T_p - F_y R_p \tag{1}$$

$$I_g\ddot{\theta}_g = T_g - F_y R_g \tag{2}$$

$$m_p\ddot{y}_p + C_{py}\dot{y}_p + K_{py}y_p = -F_y \tag{3}$$

$$m_g\ddot{y}_g + C_{gy}\dot{y}_g + K_{gy}y_g = -F_y \tag{4}$$

$$m_p\ddot{z}_p + C_{py}\dot{z}_p + K_{py}z_p = -F_z \tag{5}$$

$$m_g\ddot{z}_g + C_{gy}\dot{z}_g + K_{gy}z_g = -F_z \tag{6}$$

where I_p and I_g are pinion and gear moment of inertia, m_p and m_g are pinion and gear mass, θ_p and θ_g are pinion and gear axial rotation, respectively, y_p, y_g, z_p,

and z_g are displacements of pinion and gear along y and z axes, and superscripts ($\dot{}$) and ($\ddot{}$) show the first and the second derivatives concerning time. K_{py}, K_{gy}, C_{py}, and C_{gy} are pinion and gear bearings stiffness and damping ratio, T_p and T_g are, respectively, the exerted torques to the pinion and gear, R_p and R_g are the pinion and gear base radius, and F_y and F_z are the gear pair
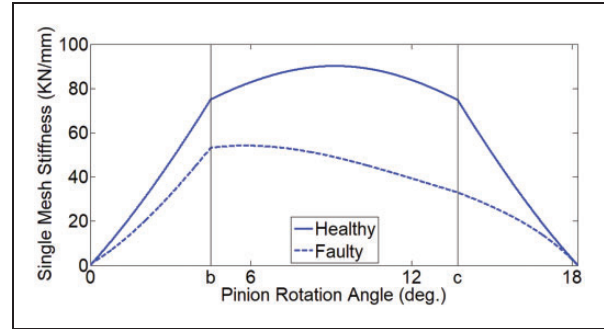
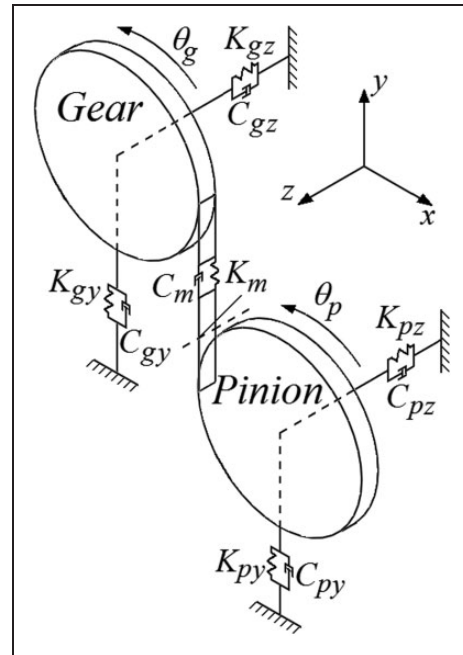**Figure 3.** Comparison of healthy and faulty tooth single stiffness.

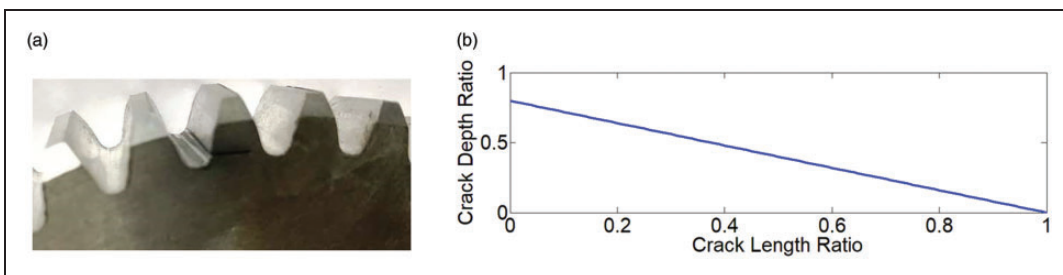**Figure 4.** Helical gear 6 DOF dynamic model.

Figure 2. (a) Tooth root crack generated by a wire-cut machine; (b) crack path in tooth length and thickness plane.

contact force components along y and z directions, respectively, computed by equations (7) to (16)

$$F_y = K_{my}\left(\tilde{y}_p - \tilde{y}_g\right) + C_{my}\left(\dot{\tilde{y}}_p - \dot{\tilde{y}}_g\right) \qquad (7)$$

$$F_z = K_{mz}\left(\tilde{z}_p - \tilde{z}_g\right) + C_{mz}\left(\dot{\tilde{z}}_p - \dot{\tilde{z}}_g\right) \qquad (8)$$

$$\tilde{y}_p = y_p + R_p\theta_p \qquad (9)$$

$$\tilde{y}_g = y_g + R_g\theta_g + e(t) \qquad (10)$$

$$\tilde{z}_p = z_p + \tilde{y}_p\tan\beta \qquad (11)$$

$$\tilde{z}_g = z_g - \tilde{y}_p\tan\beta \qquad (12)$$

$$K_{my} = K_m\cos^2\beta \qquad (13)$$

$$C_{my} = C_m\cos^2\beta \qquad (14)$$

$$K_{mz} = K_m\sin^2\beta \qquad (15)$$

$$C_{mz} = C_m\sin^2\beta \qquad (16)$$

where K_m is the mesh stiffness and C_m is the mesh damping coefficient of the gear pair, and β is the helix angle. The geometric transmission error, $e(t)$, is a periodic function, and its frequency is equal to the gear meshing frequency. So, it can be expressed as a harmonic function with $e(t) = e_0\sin(\omega_m t + \varphi_e)$.[31]

Experimental test rig data analysis

The values obtained from encoders of input and output shafts are the time intervals between two encoder's pulses. As it is best known, the transmission error can be considered as follows

$$TE = R_p\theta_p - R_g\theta_g \qquad (17)$$

By differentiating the equation to time

$$\frac{dTE}{dt} = R_p\frac{d\theta_p}{dt} - R_g\frac{d\theta_g}{dt} \qquad (18)$$

The encoders have 3600 pulses, so the angular distances between every two consecutive pulses are equal to 0.1° as given below

$$d\theta_p = d\theta_g = \Delta\theta = 0.1° \qquad (19)$$

So, the transmission error speed can be obtained by

$$\frac{dTE}{dt} = \dot{TE} = \Delta\theta\left(\frac{R_p}{\Delta t_1} - \frac{R_g}{\Delta t_2}\right) \qquad (20)$$

The experimental gear pair system's transmission error speed in 10 rotations of the pinion is depicted in Figure 5. As shown, one pulse is greater than the other in each pinion rotation, repeated with a constant period. This pulse belongs to the cracked tooth.

Using the TSA method[6] on the signal of Figure 5, the system's transmission error speed in one rotation of the pinion is obtained as shown in Figure 6. As can be seen, the signal amplitude in this region increases between approximately 100° and 140° of the pinion rotation angle. A traditional useful method to extract the signal's crack effect and determine its location is the residual signal method.[10] Figure 7 shows the residual signal of the signal shown in Figure 6. The residual signal is obtained by eliminating the gear mesh frequency and its harmonics from the original signal. As shown in Figure 7, in this method, the crack location cannot be determined precisely.

Moving average method

The moving average method is presented by Kenney.[32] According to this method, a window function with a constant width moves from the start point of the signal to the endpoint, and at each point of its motion, the average of data in the window is defined as the moving average of the point. Researchers use this method with a low-width window to eliminate noise from the main signal. But this method can be
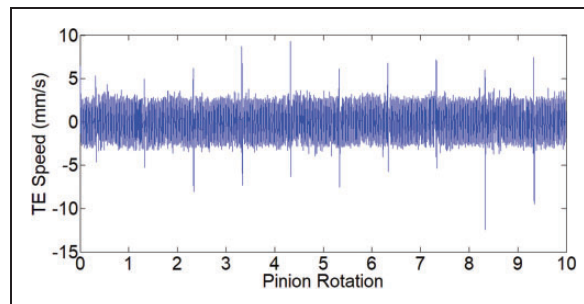
Figure 5. Transmission error speed of the experimental gear pair system in 10 rotation of the pinion.
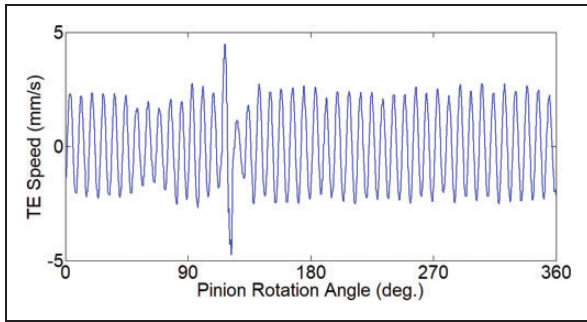
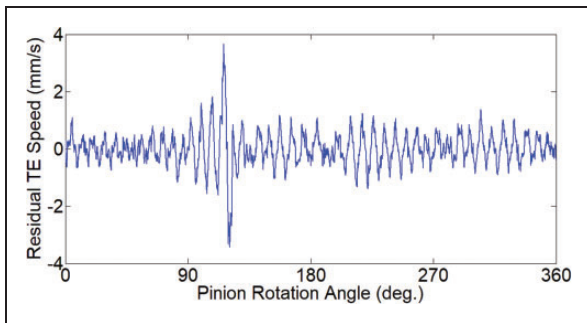**Figure 6.** The system transmission error speed in one rotation of the pinion obtained by TSA.

Figure 8. Comparison of three regions in transmission error with the same width.

Figure 7. The residual signal obtained by eliminating the gear mesh frequency and its harmonics.
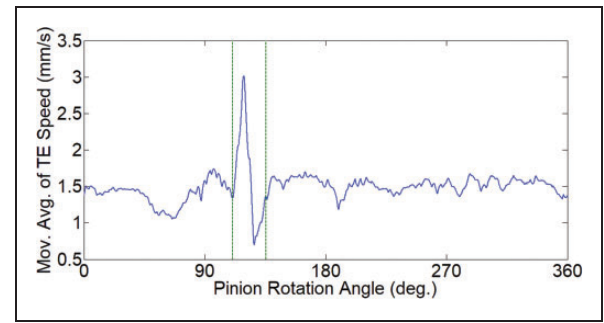
Figure 9. Start and endpoint of the crack in moving average method.

used to diagnose and find the location of local faults in periodic signals. As shown in Figure 8, in a periodic signal such as transmission error with no local faults, in various regions whose widths are equal to signal period, such as (1), (2), and (3), the average of the data in each window is equal.

So, if the moving average method with a rectangular window and the width equal to the mesh period of the gear pair is applied to the transmission error, the faults such as cracks region are determined. The window width, w, in this method can be calculated as

$$w = \frac{360}{N_1} \tag{21}$$

where N_1 is the number of teeth on the pinion. There is a problem with the resolution of the answer because of the window width. If the average value of each window refers to the center point of the window, the fault region that is determined by this method is started $\frac{w}{2}$ before the point that the real fault is started and is ended $\frac{w}{2}$ after the point that the real fault is finished, so observed sides of the crack named as α_1 and α_2 must be corrected by adding and extracting the half of window width from them, respectively
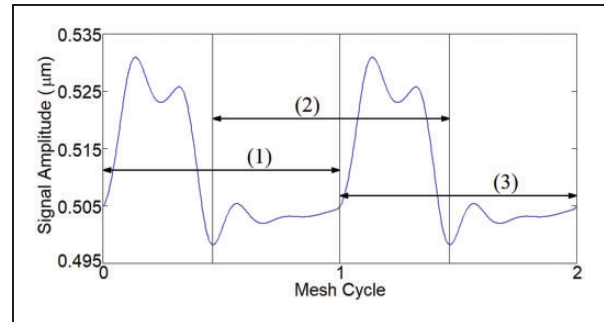
$$\alpha_{1_c} = \alpha_1 + \frac{w}{2} \tag{22}$$

$$\alpha_{2_c} = \alpha_2 - \frac{w}{2} \tag{23}$$

This method's result applied to the absolute value of the original signal presented in Figure 6 is obtained, as shown in Figure 9. According to this figure, the signal changes between two parallel vertical-dashed lines of 110.7° and 135.45° of the pinion rotation angle. The values after correction, according to equations (22) and (23), change to 114.79° and 131.36°. To detect the cracked tooth, the regions in which the pinion teeth are in contact are presented in Figure 10. According to this figure, the pinion's 15th tooth is going into contact at 114.5° and exiting contact at 132° of the pinion rotation angle, so the crack is in the 15th tooth certainly. It should be noted that the 14th and 16th teeth cannot cover the whole region of the crack effect. The crack is also a full face-width crack according to the angles obtained for the crack zone and the contact zone of the 15th tooth.

Crack depth estimation by statistical indicators

The values of some statistical indicators applied on the experimental signal are compared to the charts of those indicators obtained for various crack depth ratios, using gear pair dynamic modeling and
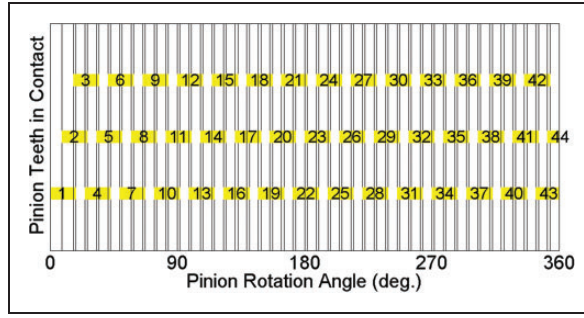
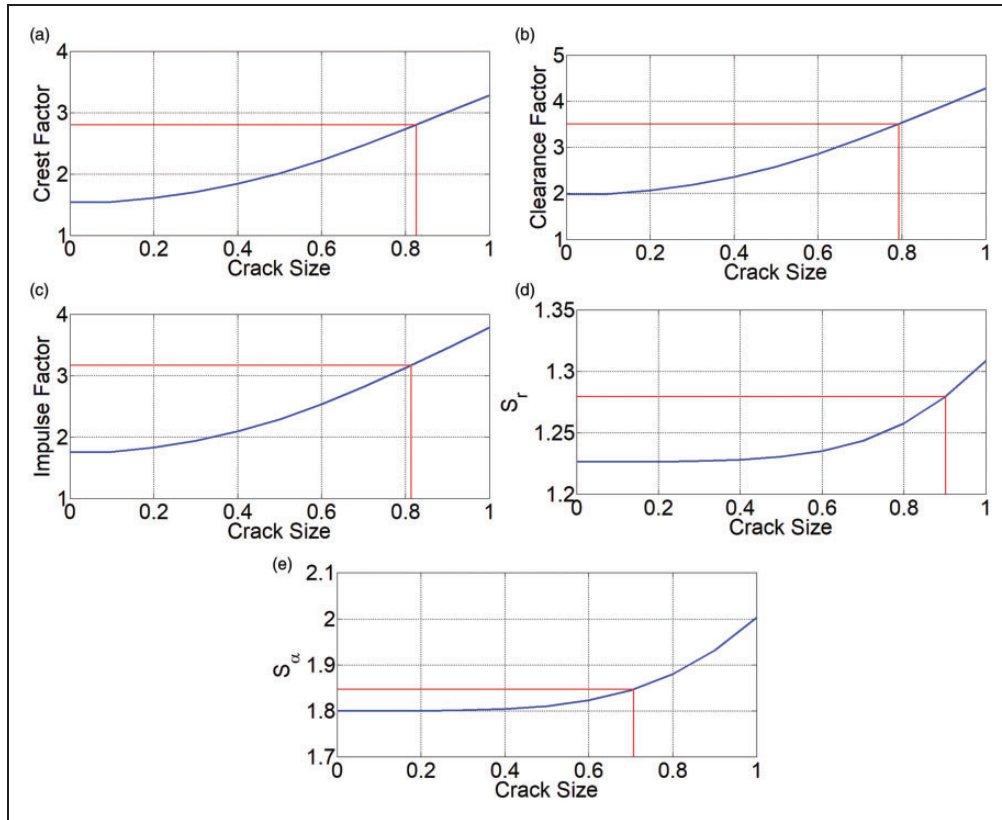**Figure 10.** The regions that the pinion teeth are in contact.

Figure 11. The results of the indicators obtained by dynamic simulation with various crack depths: (a) crest factor; (b) impulse factor; (c) clearance factor; (d) S_r; (e) S_α.

simulation to estimate the crack depth. Five indicators are selected, encompassing crest factor, impulse factor, clearance factor, S_r (third statistical moment parameter), and S_α (a statistical parameter with higher sensitivity than S_r). These indicators are dimensionless and have less sensitivity to the operating values such as load and rotation speed and more sensitivity to the faults such as cracks. The crest factor of each signal is obtained by the equation (24)[33]

$$CF = \frac{\max(|x_i|)}{RMS} \qquad (24)$$

where *RMS* is the root mean square of the signal. The equations (25) and (26) calculate the impulse factor and clearance factor, respectively[3]

$$\text{Impulse factor} = \frac{\max(|x_i|)}{\frac{1}{N}\sum_{i=1}^{N}|x_i|} \qquad (25)$$

$$\text{Clearance factor} = \frac{\max(|x_i|)}{\left(\frac{1}{N}\sum_{i=1}^{N}\sqrt{|x_i|}\right)^2} \qquad (26)$$

The equations (27) and (28) compute indicators S_r and S_α, correspondingly[4]

$$S_r = \frac{\frac{1}{N}\sum_{i=1}^{N}(x_i - \bar{x})^3}{\left(\frac{1}{N}\sum_{i=1}^{N}(x_i - \bar{x})^2\right)^{\frac{3}{2}}} \qquad (27)$$

$$S_\alpha = \frac{\frac{1}{N}\sum_{i=1}^{N}|x_i - \bar{x}|^3}{\left(\frac{1}{N}\sum_{i=1}^{N}|x_i - \bar{x}|\right)^3} \qquad (28)$$

Table 2. The estimated crack depth ratio by applying the indicators to experimental signal.

Index	Experimental value	Crack depth	Error (%)
Crest factor	2.8098	0.839	4.9
Impulse factor	3.1759	0.824	3
Clearance factor	3.5026	0.808	1
S_r	1.2798	0.909	13.6
S_α	1.8474	0.725	9.4
Estimations average	–	0.821	2.6

Results and discussion

According to Table 1, a 6 DOF dynamic model of the one-stage helical gear as presented in Figure 4 with a full face-width crack in one tooth of the pinion, Figure 2(b), with various crack depths ratio from zero to one, is solved numerically. The mentioned indicators are applied to their transmission error speed signal that is obtained by dynamic simulation. Figure 11 shows the results of these indicators. On the other hand, these indicators' values applied to the original experimental signal, Figure 6, are calculated and found at the charts' vertical axis in Figure 11. Their corresponding points along the horizontal axis show the crack depth ratio. The values of these indicators applied to the experimental signal, their estimated crack depth ratio, and the error percent of them compared to the real value of crack depth ratio are presented in Table 2. As can be seen, the crest, impulse, and clearance factors estimate the crack depth ratio with a good agreement (fewer than 5% error), and also the indicators S_r and S_α estimate it with a more significant error in comparison to the previous factors. According to equations (24) to (28), the difference between the calculated errors can be caused by each index's sensitivity to fault effects on vibration signal and their moment order of signal data. The crest, impulse, and clearance factors are the estimated crack depths, and the ratio average is 0.821, which has a 2.6% error to its real value of 0.8.

Conclusion

Helical gearboxes can be mentioned as the most applicable and fundamental systems in high-speed power transmission. It is needed to ensure that these systems are free of faults and defects because any flaw can decrease their effectiveness and lead to the rise of vibration and even operation pause. Tooth root crack is one of the most common faults happening in gears. Therefore, specific attention is paid to crack diagnosis in the gear systems. However, a review of previous research reveals that these researchers' focus is on identifying the cracks' location, and most of them have studied the spur gear pair. Also, in some experimental results, traditional methods such as residual signal cannot precisely determine the cracked tooth. So, it seems necessary to propose a new approach to find the cracked tooth and also diagnose the crack depth ratio in the helical gear pair. In this research, the dynamic responses of the one-stage helical gear system were calculated. For this purpose, the gear mesh stiffness was obtained, the modeling of the cracked tooth was described, and the crack effect on its mesh stiffness was modeled. Then, the vibration data, dynamic responses of a one-stage helical gear system were obtained by an experimental test rig, and the moving average method was used to detect the crack location. Then, using some statistical indicator charts obtained by dynamic simulation, the crack depth ratio was estimated. Finally, the accuracy of each indicator in this experimental study was discussed. The crest factor, impulse factor, and clearance factor calculated the crack depth ratio with a satisfactory agreement, and also the indicators S_r and S_α estimated it with more significant errors to the other factors. The average of the crack depth ratio's estimated values calculated and obtained a better result than each indicator alone.

The computational procedure is developed in MATLAB programming software. The running time is five minutes by a regular PC. The proposed method can be used in the gearbox test bench because the test time under load usually takes 8 h. This method can estimate the crack location and size with less accuracy for a smaller crack size. If the crack size was too small and its effect on vibration signal became smaller than other real and spurious vibration sources, this method could not find it.

Generally, temperature, the gearbox case vibrations in three directions, and generated noise are standard criteria for fault detection in the gearbox monitoring benches and on-site. As mentioned before, the presented method can be used in gearbox test benches to estimate the location and size of the crack. The crack effect on mesh stiffness could affect other vibration signals, such as lateral vibrations on input and output shafts. Therefore, on-site, the inspector can monitor the crack defect by attaching some vibrometers or accelerometers to the gearbox case in the right place and direction on-site.

As presented in "Moving average method" section, if a fault signal remains in a tooth zone, it can be related to a tooth's fault. According to experience, if fault signals are observed in several teeth, it can

be gear tooth pitting. But suppose there is a tooth local fault such as tooth pitting or a tooth broken edge generated a similar dynamic signal as a tooth root crack, there is no way to recognize that this signal is caused by a crack or other faults.

Declaration of conflicting interests

The author(s) declared no potential conflicts of interest with respect to the research, authorship, and/or publication of this article.

ORCID iDs

Mohsen Rezaei https://orcid.org/0000-0002-8805-477X
Mehrdad Poursina https://orcid.org/0000-0002-9974-9702

References

1. Mohammed OD. *Dynamic modelling and vibration analysis for gear tooth crack detection*. PhD Thesis, Luleå Tekniska Universitet, 2015.
2. Sait AS and Sharaf-Eldeen YI. A review of gearbox condition monitoring based on vibration analysis techniques diagnostics and prognostics. *Rotat Mach Struct Health Monit* 2011; 5: 307–324.
3. Alkhadafe H, Al-Habaibeh A and Lotfi A. Condition monitoring of helical gears using automated selection of features and sensors. *Measurement* 2016; 93: 164–177.
4. Wu S, Zuo MJ and Parey A. Simulation of spur gear dynamics and estimation of fault growth. *JSV* 2008; 317: 608–624.
5. Skrickij V, Bogdevičius M and Junevičius R. Diagnostic features for the condition monitoring of hypoid gear utilizing the wavelet transform. *Appl Acoust* 2016; 106: 51–62.
6. Jardine AK, Lin D, Banjevic D. A review on machinery diagnostics and prognostics implementing condition-based maintenance. *MSSP* 2006; 20: 1483–1510.
7. Barszcz T and Randall RB. Application of spectral kurtosis for detection of a tooth crack in the planetary gear of a wind turbine. *MSSP* 2009; 23: 1352–1365.
8. Dalpiaz G, Rivola A and Rubini R. Effectiveness and sensitivity of vibration processing techniques for local fault detection in gears. *MSSP* 2000; 14: 387–412.
9. Braun S. The synchronous (time domain) average revisited. *MSSP* 2011; 25: 1087–1102.
10. Combet F, Gelman L, Anuzis P, et al. Vibration detection of local gear damage by advanced demodulation and residual techniques. *PIG* 2009; 223: 507–514.
11. Mohammed OD, Rantatalo M and Aidanpää JO. Dynamic modelling of a one-stage spur gear system and vibration-based tooth crack detection analysis. *MSSP* 2015; 54: 293–305.

12. Amarnath M and Krishna IP. Local fault detection in helical gears via vibration and acoustic signals using EMD based statistical parameter analysis. *Measurement* 2014; 58: 154–164.
13. Assaad B, Eltabach M and Antoni J. Vibration based condition monitoring of a multistage epicyclic gearbox in lifting cranes. *MSSP* 2014; 42: 351–367.
14. Zhou X, Shao Y, et al. Time-varying meshing stiffness calculation and vibration analysis for a 16DOF dynamic model with linear crack growth in a pinion. *J Vib Acoust* 2012; 134: 011011.
15. Randall RB, Sawalhi N and Coats M. A comparison of methods for separation of deterministic and random signals. *IJCM* 2011; 1: 11–19.
16. Elasha F, Ruiz-Carcel C, Mba D, et al. A comparative study of the effectiveness of adaptive filter algorithms, spectral kurtosis and linear prediction in detection of a naturally degraded bearing in a gearbox. *JFAP* 2014; 14: 623–636.
17. Furch J, Nguyen TT and Glos J. Diagnostics of gear fault in four-speed gearbox using vibration signal. In: *2017 International conference on military technologies (ICMT)* (ed. Krivanek, Vaclav), 31 May 2017, pp.87–92. Piscataway, NJ: IEEE.
18. Wu J, Yang Y, Yang X, et al. Fault feature analysis of cracked gear based on LOD and analytical-FE method. *MSSP* 2018; 98: 951–967.
19. Liang X, Zuo MJ and Liu L. A windowing and mapping strategy for gear tooth fault detection of a planetary gearbox. *MSSP* 2016; 80: 445–459.
20. Omar FK and Gaouda AM. Gear tooth diagnosis using wavelet multi-resolution analysis enhanced by Kaiser's windowing. *TIM* 2011; 33: 573–590.
21. Parey A and Pachori RB. Variable cosine windowing of intrinsic mode functions: application to gear fault diagnosis. *Measurement* 2012; 45: 415–426.
22. D'Elia G, Mucchi E and Dalpiaz G. On the time synchronous average in planetary gearboxes. *Int Conf-Surveil* 2013; 7: 1–11.
23. Wang Z, Guo Y and Wu X. Sun gear fault diagnosis based on windowed synchronous average in angle domain. In: *2016 IEEE international conference on information and automation (ICIA)I* (ed. MENG Q., H. Max), 1 August 2016, pp.785–790. Piscataway, NJ: IEEE.]
24. Wang Z, Guo Y, et al. Localized fault detection of sun gears based on windowed synchronous averaging in the angular domain. *Advances in Mechanical Engineering* 2017 Mar; 9(3). DOI:1687814017696412.
25. Rezaei M, Poursina M, Jazi SH, et al. Multi crack detection in helical gear teeth using transmission error ratio. *JMST* 2019; 33: 1115–1121.
26. Mohammed OD and Rantatalo M. Gear fault models and dynamics-based modelling for gear fault detection- a review. *Eng Failure Anal* 2020; 117: 104798.
27. Luo W, Qiao B, Shen Z, et al. Investigation on the influence of spalling defects on the dynamic performance of planetary gear sets with sliding friction. *Tribol Int* 2021; 154: 106639.
28. Chen Y, et al. A time series model-based method for gear tooth crack detection and severity assessment under random speed variation. *MSSP* 2021; 156: 107605.

29. Chen Z, Zhai W and Wang K. Vibration feature evolution of locomotive with tooth root crack propagation of gear transmission system. *MSSP* 2019; 115: 29–44.

30. Wan Z, Cao H, et al. Mesh stiffness calculation using an accumulated integral potential energy method and dynamic analysis of helical gears. *Mech Mach Theory* 2015; 92: 447–463.

31. Yang Y, Xia W, et al. Vibration analysis for tooth crack detection in a spur gear system with clearance nonlinearity. *IJMS* 2019; 157: 648–661.

32. Kenney JF. Moving averages. *Math Stat* 1962; 1: 221–223.

33. Samuel PD and Pines DJ. A review of vibration-based techniques for helicopter transmission diagnostics. *JSV* 2005; 282: 475–508.